Published online 2 September 2008 *Nucleic Acids Research, 2008, Vol. 36, No. 17* ***5623–5634***
doi:10.1093/nar/gkn533

DNA replication timing is deterministic at the level of chromosomal domains but stochastic at the level of replicons in *Xenopus* egg extracts

Hélène Labit, Irène Perewoska, Thomas Germe, Olivier Hyrien and Kathrin Marheineke*

Ecole Normale Supérieure, Biology Department, Laboratory of Molecular Genetics, CNRS UMR 8541, 46, rue d'Ulm, 75005 Paris, France

Received April 11, 2008; Revised August 1, 2008; Accepted August 4, 2008

ABSTRACT

Replication origins in *Xenopus* egg extracts are located at apparently random sequences but are activated in clusters that fire at different times during S phase under the control of ATR/ATM kinases. We investigated whether chromosomal domains and single sequences replicate at distinct times during S phase in egg extracts. Replication foci were found to progressively appear during early S phase and foci labelled early in one S phase colocalized with those labelled early in the next S phase. However, the distribution of these two early labels did not coincide between single origins or origin clusters on single DNA fibres. The 4 Mb *Xenopus* rDNA repeat domain was found to replicate later than the rest of the genome and to have a more nuclease-resistant chromatin structure. Replication initiated more frequently in the transcription unit than in the intergenic spacer. These results suggest for the first time that in this embryonic system, where transcription does not occur, replication timing is deterministic at the scale of large chromatin domains (1–5 Mb) but stochastic at the scale of replicons (10 kb) and replicon clusters (50–100 kb).

INTRODUCTION

Eukaryotic DNA replication requires a strict control of origin density and origin firing time. Origins are 'licensed' for replication by the loading of Mcm 2–7 proteins on chromatin in late mitosis and G1, thus forming pre-replicative complexes (pre-RCs). Pre-RCs are subsequently activated during S phase by cyclin- and Dbf4/Drf1-dependent kinases (CDKs and DDKs), which leads to the recruitment of many other factors, DNA unwinding and start of DNA synthesis at origins (1). Origins are not all fired at the same time but follow a staggered programme of activation. In budding yeast, where origins are well identified, *cis*-acting sequences that control origin firing time have been identified and in most cases, these sequences are separable from those that control origin activity (2). Some of these determinants appear to exert their effects through modulation of chromatin structure and can influence origin firing time over significant distances. A recent study showed that the apparently precise temporal programme deduced from examination of cell populations (3) is in fact probabilistic: when individual yeast chromosome VI molecules were examined by DNA combing, no two molecules exhibited the same replication pattern (4).

In most metazoan cells, replication also initiates at fairly specific sites and chromosomal domains replicate following a defined spatio-temporal programme (5). DNA synthesis takes place at different types of intranuclear replication foci during different stages of S phase, and this pattern is reproducible from one cell cycle to the next. These replication timing domains are thought to form distinct, stable units of chromosomal structure that encompass synchronous replicons and localize to specific nuclear compartments. Although *cis*-acting determinants of replication time have not been defined in metazoans, it has long been recognized that transcriptionally active domains replicate before transcriptionally silent domains, although this correlation is not absolute (5). A recent genomic study in *Drosophila* showed that the correlation between early replication and RNA Pol II occupancy is strongest over large domains (~180 kb) including many genes, rather than over individual genes (6). In mammals, the replication timing of chromosomal domains is established early during the G1 phase, simultaneously with their specific repositioning in the nucleus after mitosis (7). The 'timing decision point' occurs after replication licensing but prior to the 'origin decision point' in mid-G1, when origin specification is acquired (8).

*To whom correspondence should be addressed. Tel: +33 1 44 32 37 33; Fax: +33 1 44 32 39 41; Email: marheine@biologie.ens.fr
Present addresses:
Hélène Labit, Marie Curie Research Institute, The Chart, Oxted, Surrey RH8 0TL, UK
Thomas Germe, London Research Institute, 44 Lincoln's Inn Fields, London WC2 3PX, UK

This observation underlines that genomes can replicate with an organized timing but without a defined pattern of origin firing (9).

An important but unanswered question is whether early vertebrate embryos have a replication timing programme similar to that observed in adult somatic cells. The early *Xenopus* embryo has an abbreviated cell cycle (~30 min) with no transcription and no distinct G1 and G2 phases (10). Furthermore, the number, size and distribution of replication foci seem to remain roughly constant throughout S phase when sperm nuclei are replicated in *Xenopus* egg extracts, in stark contrast with the temporal succession of different types of replication foci observed during S phase in adult somatic cells (11). The lack of G1 phase, transcription and temporal subtypes of replication foci, raises the possibility that there is no replication timing programme in *Xenopus* embryos or egg extracts.

One possibility is that a replication timing programme is only established at the midblastula transition (MBT), when transcription resumes in the embryo. It has been shown that replication initiates at apparently random sequences spaced at ~10 kb intervals in early embryos (12) or egg extracts (13–15), but at specific sites after the MBT (16). Subsequent single molecule studies have clearly shown that replication origins fire at different times throughout S phase in *Xenopus* egg extracts (15,17–20). Although this could be consistent with stochastic initiation, it was also found that adjacent replication bubbles tend to be of similar sizes in egg extracts, suggesting the existence of synchronously activated clusters of 5–10 origins, as in adult somatic cells (17,20,21). Random initiation cannot produce such correlations. One possibility is that initiation at one origin enhances the likelihood of nearby initiations (21). Alternatively, some event distinct from initiation may render a stretch of 5–10 origins more likely to initiate (20). Increasing the concentration of nuclei in the extracts spreads the time period over which different clusters fire, without altering origin spacing within clusters, whereas ATM/ATR inhibition compresses this time period (20). These findings raise the possibility that a defined replication timing programme may exist before the MBT, in the absence of a defined spatial pattern of origin firing. Yet, it remains possible that origin clusters are activated in a stochastic manner.

In order to further explore the replication timing programme in *Xenopus* embryos, we have used deconvolution microscopy to show that replication foci are activated in a discernibly progressive manner during early S phase upon incubation of sperm nuclei in egg extracts. We have exploited this system to ask further whether replication foci labelled at the beginning of one S phase are also labelled at the beginning of the next. We have investigated at the single molecule level on combed DNA fibres whether genomic DNA sequences labelled at the beginning of two consecutive S phases would coincide. We further asked whether a specific 4 Mb chromosomal domain on chromosome XII, the *Xenopus* rDNA domain, replicates at a different time than the rest of the genome and we have re-examined the pattern of origin firing at this locus. Our results show for the first time that replication timing in *Xenopus* egg extracts is deterministic, and independent of ATM/ATR, at the level of large chromosomal domains in the absence of transcription, but stochastic (and ATM/ATR dependent) at the level of origins and origin clusters.

MATERIALS AND METHODS

Replication of sperm nuclei in *Xenopus* egg extracts

Interphase egg extracts were prepared as described before (19). Demembranated sperm nuclei were incubated (at 200–2000 nuclei/μl) in extracts supplemented with an energy regeneration mix (7.5 mM creatine phosphate, 1 mM ATP, 0.1 mM EGTA pH 7.7, 1 mM $MgCl_2$), creatine kinase (100 μg/ml), cycloheximide (250 μg/ml). For analysis of replication foci, 33 μM rhodamine–dUTP (Roche Applied Science, Basel, Switzerland) was added at the indicated times for 2 min and the reaction was stopped with 1 × PBS and fixed in 4% *p*-formaldehyde. For analysis of the rDNA locus, sperm nuclei (500 nuclei/μl) were incubated in extracts in the presence of energy mix, cycloheximide and 14.3 μM digoxigenin–dUTP (Roche Applied Science) and chased with 2 mM dTTP at the indicated times.

For cycling extracts experiments sperm nuclei (100 nuclei/μl) were incubated in fresh cycling extracts supplemented with energy mix and cytochalasin B (10 μg/ml) in the absence of cycloheximide. The kinetics of entry into mitosis was monitored by direct fluorescence microscopy of an aliquot of the same nuclei in the same extract. DNA synthesis was assessed in both rounds of replication by measuring incorporation of [α-^{32}P]dATP. Aliquots were diluted in 6 volumes of 1% SDS, 40 mM EDTA, 300 mM NaCl. Samples were digested with RNase A and proteinase K and electrophoresed without extraction. Gels were dried, exposed to Film Imaging Plates and analysed on a Fluorescent Image Analyzer FLA-3000 (Fujifilm, Tokyo, Japan). For colocalization of replication foci in two subsequent S phases, foci were labelled in the first S phase with 33 μM rhodamine–dUTP at 16 min for 2 min followed by a chase of 2 mM dTTP. Mitotic entry was monitored by nuclear morphology in the presence of Hoechst (Sigma, St. Louis, MO, USA). Foci were labelled in the second S phase with 33 μM biotin–dATP at 65–80 min, before reactions were stopped and fixed. Biotin-labelled foci were revealed with streptavidin Alexa Fluor 488 (Molecular Probes, Invitrogen, Carlsbad, CA, USA). For combing experiments the first round of replication was pulse labelled with 20 μM digoxigenin–dUTP (Roche Applied Science) (added at $t = 0$) and chased with 1.33 mM dTTP at 24 min. The second round of replication was pulse labelled with 20 μM biotin–dATP (Perkin Elmer, Waltham, MA, USA) (added at $t = 1$ h) and chased with 2 mM dATP at 90 min.

Molecular combing and detection by fluorescent antibodies

Labelled DNA was extracted and combed as described (18) on silanized glass coverslips produced by liquid-phase silanization (Labit *et al*., submitted for publication).

For analysis of early replication in two successive rounds of replication, fluorescent detection and signal

amplification of both digoxigenin and biotin labels were simultaneously performed using five successive layers of fluorochrome-conjugated antibodies: (i) Alexa Fluor 594 streptavidin (Molecular Probes, Invitrogen) and mouse anti-digoxin-FITC (Interchim, Montluçon, France), (ii) biotinylated anti-streptavidin (Molecular Probes, Invitrogen) and donkey anti-mouse-FITC (Interchim), (iii) Alexa Fluor 594 streptavidin and F1 (anti-FITC; Cambio, Cambridge, UK), (iv) biotinylated anti-streptavidin and F2 (anti-anti-FITC; Cambio), (v) Alexa Fluor 594 streptavidin. Total DNA was stained at room temperature for 30 min with 1:7000 YOYO-1 1 mM (Molecular Probes, Invitrogen) in PBS before rinsing 5 min in PBS and mounting in Vectashield®. Alternatively, when specifically mentioned, total DNA was detected with a mouse anti-DNA antibody (Abcys, Paris, France) followed by rabbit anti-mouse Alexa Fluor 488 and goat anti-rabbit Alexa Fluor 488 antibodies (Molecular Probes, Invitrogen).

To assess the global replication extent in the rDNA analysis, total DNA was detected using a mouse anti-guanosine antibody (Argene, Varilhes, France) followed by anti-mouse Alexa Fluor 594 (Molecular Probes, Invitrogen).

Digestion of chromatin with micrococcal nuclease

Micrococcal nuclease (Roche Applied Science) digestion of sperm chromatin incubated in egg extracts supplemented with geminin was performed as described (22).

Hybridizations

For FISH experiments on combed fibres two different restriction fragments were used as probes. The probe called B is a 4787 bp EcoRI restriction fragment at the 3′-end of the *Xenopus* gene coding the 40 S rRNA precursor, the probe A is a 8560 bp EcoRI restriction fragment corresponding to the intergenic spacer and the 5′-end of the rDNA gene (12). Fragments were biotinylated or digoxigenylated using the BioPrime® DNA Labelling System (Invitrogen, Carlsbad, CA, USA).

Hybridizations were carried out using 250 ng of probe per slide as described (23) and digoxigenin and biotin labels were consecutively detected with nine successive layers of the fluorochrome-conjugated antibodies described above.

Southern blotting of chromatin reactions digested with micrococcal nuclease was performed as described (22). Hybridization was carried out with a probe corresponding to the full *Xenopus* rDNA gene and the intergenic spacer (12).

Imaging

Images of nuclei and combed DNA fibres were acquired using a 100×, 1.4 numerical aperture UPlanSApo objective on an Olympus IX 81 inverted microscope connected to a CoolSNAP HQ CCD camera (Photometrics, Tuscon, AZ, USA) run by MetaMorph version 6.3r7 (Molecular Devices, Union City, CA, USA). Images were processed either with Adobe Photoshop CS2 (Adobe Systems Inc., San Jose, CA, USA) or ImageJ (Rasband, 1997–2007). For foci analysis Z stacks (30) per nuclei were acquired at 0.2 μm interval. Images were processed in ImageJ using the Z projection function, convolution filter and a 2D iterative deconvolution function. Replication foci of 50 randomly chosen nuclei were counted on deconvoluted images after automated thresholding.

For colocalization analysis 50 nuclei showing early replication pattern with both rhodamine–dUTP and biotin–dATP labelling were analysed. A modified Pearson coefficient for images of both channels was determined as described in (24) and the percentage of colocalization was calculated using Matlab 5.3 (The MathWorks Inc., Natick, MA, USA) for the 50 nuclei.

Measurements of combed DNA and data analysis

The fields of view were chosen at random unless mentioned otherwise. Measurements on each molecule were made using Image Gauge version 4.2 (Fujifilm) and compiled using Microsoft Excel (2004). Replication eyes were defined as the incorporation tracks of either digoxigenin–dUTP or biotin–dATP. No lower limit of detection had to be defined because the background staining was very low. Replication eyes were considered as the products of two replication forks whereas incorporation tracks at the extremities of DNA fibres were considered as the products of one replication fork. Fork density was obtained by dividing total DNA by the total number of forks. The midpoints of replication eyes were defined as the origins of replication. Eye-to-eye distances (ETED), also known as inter-origin distances, were measured between the midpoints of adjacent replication eyes. Incorporation tracks at the extremities of DNA fibres were not regarded as replication eyes but were included in the determination of the global incorporation extent calculated as the sum of incorporation divided by total DNA. Distributions of ETED were made into classes of 5 kb and plotted using Origin® version 6.0 (OriginLab, Northampton, MA, USA).

RESULTS

The number of replication foci changes during S phase progression in sperm nuclei

In animal cells, DNA replication takes place in subnuclear domains known as replication foci, which show reproducible changes in size, number and position during S phase. In the *Xenopus in vitro* system it was reported that replication initiates at discrete foci whose pattern remains unchanged throughout S phase (11). Since we and others have shown that origins fire throughout S phase in this embryonic system (15,17–20), we investigated whether a temporal programme of replication foci can be detected in sperm nuclei replicated in egg extracts.

Replication foci in sperm nuclei replicating in *Xenopus* egg extracts were visualized by high resolution fluorescence microscopy after short pulses of rhodamine–dUTP early and late in S phase. At the onset of S phase (16 min) we observed three different patterns of label incorporation due to the slight asynchronous entry into S phase: few punctuate foci (Figure 1A), many punctuate foci (Figure 1B and C) and bright nuclei whose individual

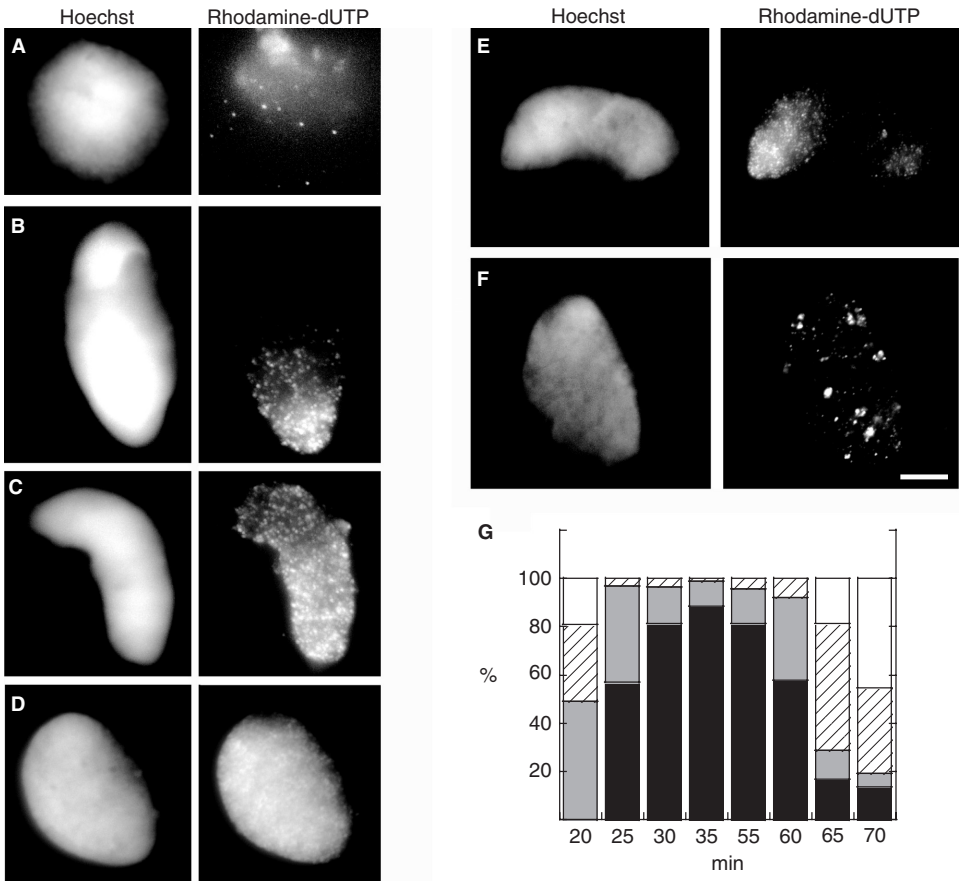

Figure 1. Different replication patterns of sperm nuclei in *Xenopus* egg extracts. (**A**–**F**) Examples of representative foci patterns. Sperm nuclei were labelled early (**A**–**D**, at 16 min) or late (**E** and **F**, at 65 min) in S phase by incorporation of rhodamine–dUTP for 2 min (Z projections of 30 stacks at 0.2 μm interval), bar = 3 μm. (**G**) After pulse labelling of nuclei throughout S phase with rhodamine–dUTP, the different patterns of replication foci were scored (150 nuclei per time point; white: no foci, lines: few foci, grey: many punctuate foci, black: uniform staining).

foci were too numerous to be resolved (Figure 1D). Very late in S phase (65 min), discrete foci became again visible (Figure 1E and F). We also found variations in the size and distribution of foci: discrete foci polarized at one end of the nucleus (Figure 1B) were observed in ~5% of total nuclei in both early and late S phase (their percentage varied between experiments). Some nuclei also presented few large foci scattered among a majority of smaller foci late in S phase (Figure 1F). To determine if the three patterns (few punctuate, many punctuate and bright) represented nuclei having progressed through S phase to different extents, their percentages were counted at different stages of S phase (Figure 1G). Nuclei with few or many individual foci predominated during very early S phase; they were quickly replaced by uniformly labelled nuclei by mid S phase and only reappeared late in S phase. This temporal succession of patterns suggests that under our experimental conditions, we are able to resolve the progressive activation and disappearance of replication foci during early and late S phase, respectively, and that foci are too numerous and/or too bright in mid S phase to be resolved.

To obtain more precise quantifications, replication foci were counted next on deconvoluted images after Z-stack projections (Figure 2A). Nuclei were pulse labelled with rhodamine–dUTP at two early (17 and 20 min) and two late (65 and 70 min) time points in S phase. The number of foci per nucleus increased from a few up to maximal 250 foci per nucleus early in S phase and decreased again late in S phase (Figure 2B). We next asked whether the ATM/ATR inhibitor caffeine affected the activation of replication foci in very early S phase. No significant effect of caffeine on the number of foci was observed ($P = 0.35$; Mann–Whitney test, Figure 2C). However, the mean pixel intensities of nuclei were higher in the presence of caffeine (data not shown), in agreement with the previously reported effect of caffeine on the rate of DNA synthesis (20,25).

We conclude that the number of replication foci increases and decreases progressively, independent of ATR/ATM kinase activity, at the beginning and at the end of S phase in the *Xenopus in vitro* system.

Replication foci are activated in a deterministic order

Having shown that replication foci are activated in a progressive manner during early S phase, we examined if this order was reproducible between two successive S phases in cycling egg extracts, which are able to perform several rounds of alternating S and M phases (26). Sperm nuclei were pulse labelled at the beginning of the first S phase

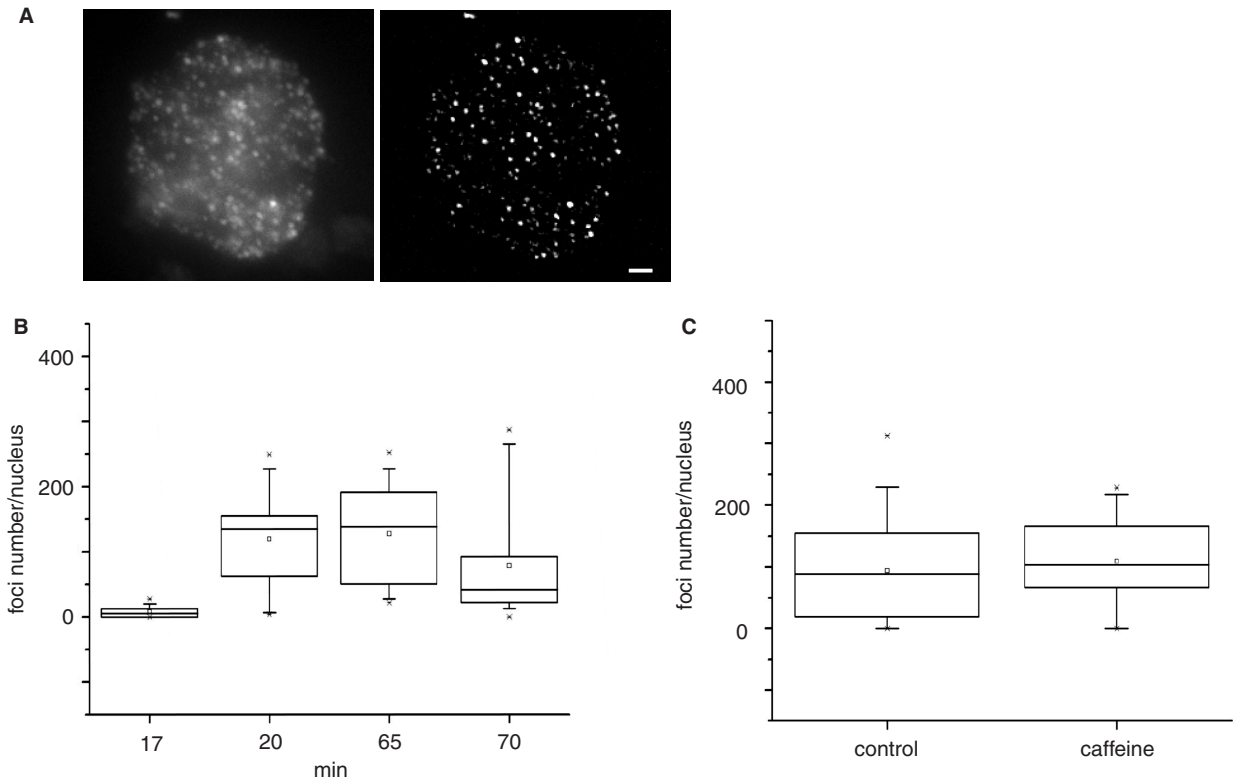

Figure 2. The number of replication foci changes during S phase in *Xenopus* egg extracts. (**A**) Example nuclei labelled early with rhodamine–dUTP before (Z projection of 30 stacks, left) and after (right) deconvolution, bar = 1 μm. (**B**) Early and late replication foci in 50 nuclei were counted on deconvoluted images. Results are shown as box-and-whisker plots with vertical lines indicating the 98% range, boxes the 25–75th percentile and black horizontal lines the mean. (**C**) Box-and-whisker plots of the number of early (t = 16 min) replication foci in control and caffeine (5 mM) treated samples.

with digoxigenin–dUTP, chased with dTTP and pulsed labelled again with biotin–dATP at the beginning of the second S phase (Figure 3A). The kinetics of entry into the intervening mitosis was simultaneously monitored by direct fluorescence microscopy to control that the second label was added at the appropriate time. No incorporation of biotin–dATP was observed when entry into mitosis was prevented using cycloheximide (data not shown). However, in cycling extracts we observed a high degree of colocalization of the two labels within one nucleus, showing that the first active foci at the beginning of one S phase were also the first to be activated at the beginning of the next (Figure 3B–I). In order to quantify the colocalization of replication foci between two S phases we analysed 50 nuclei showing early S phase replication pattern. The distribution of colocalization values fitted a Gaussian distribution and a mean of 92% (±6.9%) colocalization was calculated (Figure 3J). This experiment shows that the temporal order of foci appearance is maintained from one cell cycle to the other. We conclude that foci are activated in a non-random, thus deterministic order in *Xenopus* egg extracts.

Replication origin firing time is not predetermined on the single origin level

We next investigated whether the colocalization of labels incorporated at the beginning of two consecutive S phases, as observed at the level of replication foci, could also be observed at the level of origins and origin clusters on combed DNA fibres. Early firing replication origins in the first S phase were labelled by a pulse of digoxigenin–dUTP, followed by a chase with dTTP (t = 0–24 min), and early firing origins in the second S phase were labelled by a pulse of biotin–dATP, followed by a chase with dATP (t = 60–90 min) (Figure 4A). Several control experiments were performed in parallel. First, the kinetics of entry into mitosis was simultaneously monitored by fluorescence microscopy of whole nuclei in the presence of Hoechst. Second, replication kinetics was monitored by [α-^{32}P]dATP incorporation (Figure 4B) and by DNA combing in both rounds (not shown). Both S phases were found to be efficient (>50%). The clear plateau of incorporation between 45 and 75 min shows that biotin–dATP was neither added too early nor too late in order to label origins in the second S phase. Third, in order to exclude that some nuclei had not finished replication at the time of biotin–ATP addition, its incorporation was assessed in the presence of cycloheximide, which prevents exit from the first interphase. We found that biotin–dATP incorporation on single fibres was negligible. Finally, incorporation of digoxigenin–dUTP in the first S phase had no effect on the cycling kinetics and the incorporation of biotin–dATP during the second S phase (data not shown).

The extent of digoxigenin–dUTP and biotin–dATP incorporation on combed DNA fibres was 12.1 and 8.3%, respectively, and the mean replication eye lengths

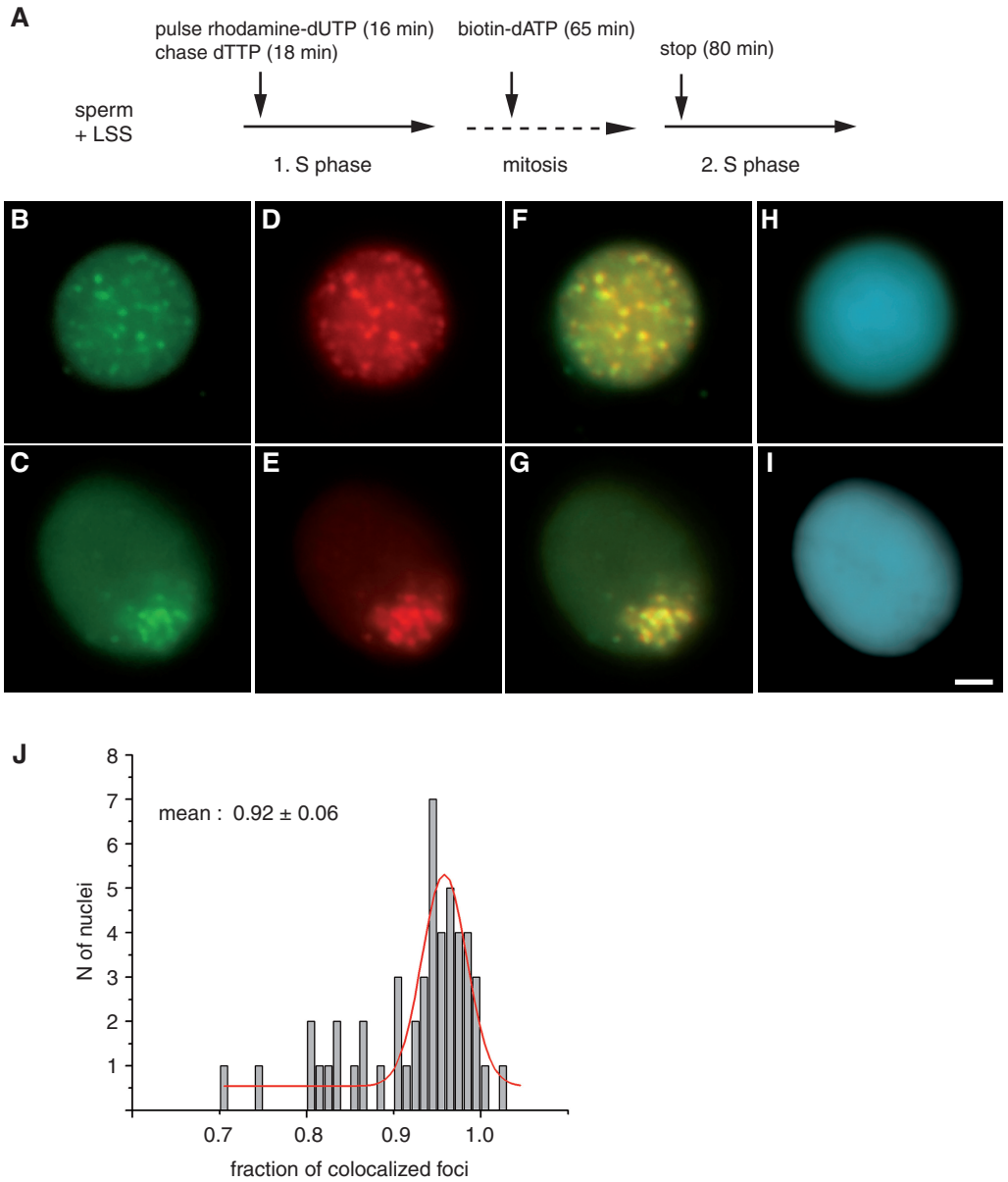

Figure 3. Colocalization of replication foci in two successive S phases in cycling extracts. (**A**) Labelling scheme: sperm nuclei (100 nuclei/μl) were incubated in egg extracts low speed supernatant (LSS) in the absence of cycloheximide, pulse labelled early in the first S phase with rhodamine-dUTP (16–18 min, red) and early in the second S phase with biotin-dATP (65–80 min, green). Replication foci in two different nuclei labelled in the first S phase (**B** and **C**), second S phase (**D** and **E**), merged images of first and second S phases (**F** and **G**), Hoechst (**H** and **I**), bar = 2 μm. (**J**) Quantitative colocalization analysis: the fraction of colocalized foci was calculated from 50 nuclei. Red curve shows a fitted Gaussian distribution.

(3.17 kb versus 3.74 kb) and other replication parameters were similar between the two S phases (Figure 4C, Table 1). DNA replication was analysed on a selected subset of fibres containing at least one origin fired in each S phase (Figure 4A and C). Assuming that the sequences that are replicated during early S phase in two successive cycles do not coincide more than expected by chance, the extent of overlap of the red and green signals should be $0.121 \times 0.083 = 1.00\%$. The measured extent of overlap (yellow pixels) was 1.15%, not significantly different from that expected by chance alone. Therefore, sequences that are used as early origins in one S phase are not preferentially used as early origins in the next one.

Since no coincidence between individual origins was observed we next asked whether there was coincidence at the level of origin clusters between two S phases. We compared the distances between origins activated during either the first (ETEDdig) or the second (ETEDbio) round of replication with the distances between all origins activated in the first and second S phases (ETEDdigbio). If the same origin clusters were activated in the two different S phases, the red origins should intersperse with the green ones. This would result in ~2-fold shorter distances between origins when both labels are recorded rather than a single one. On the other hand, if early clusters of the first and second S phases were exclusive sets, the distribution of inter-origin

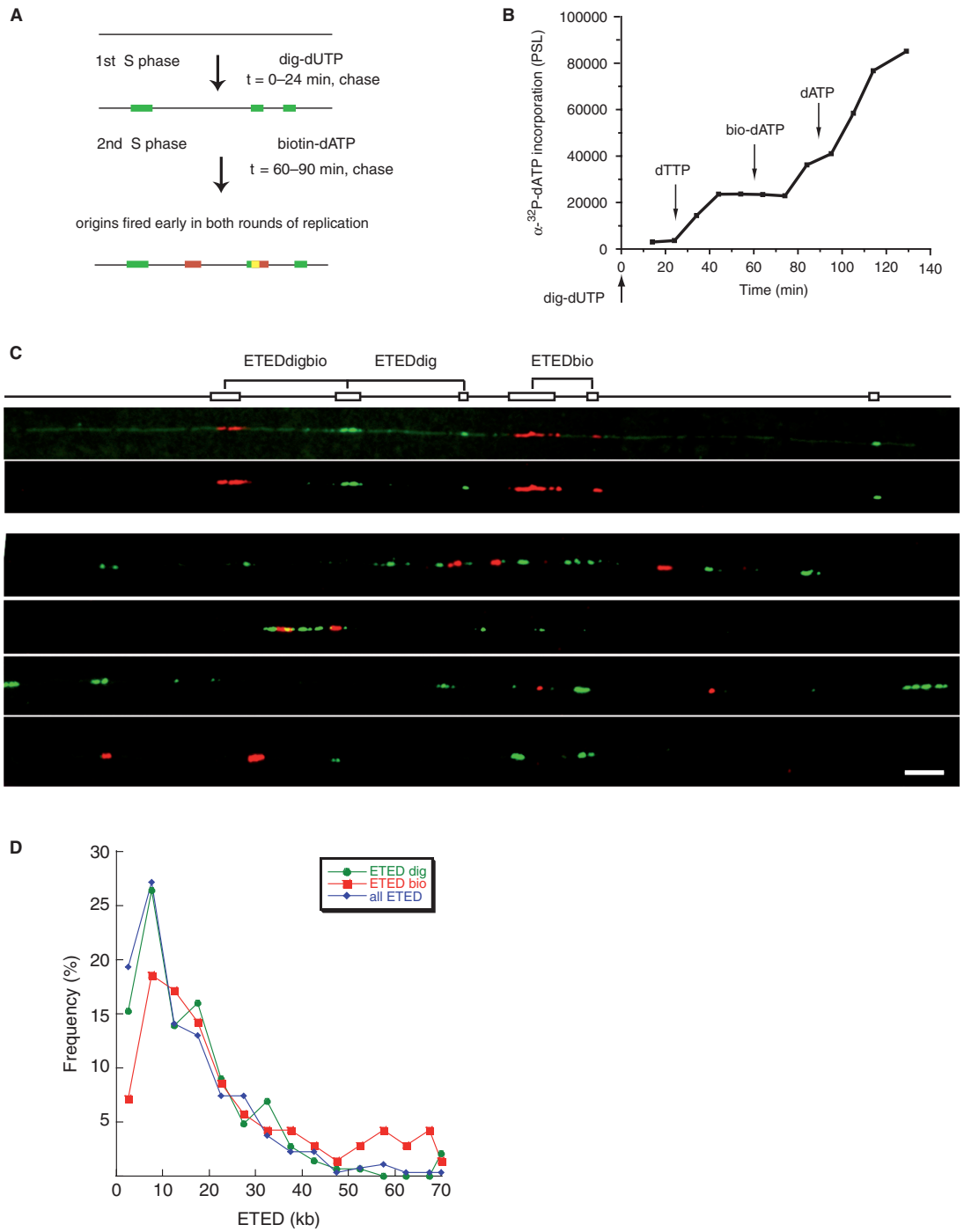

Figure 4. Activation of origins in two successive S phases. (**A**) Labelling scheme for colocalization of origins used in two consecutive S phases by DNA combing. (**B**) Replication kinetics: sperm nuclei were incubated at 100 nuclei/µl in cycling egg extracts in the presence of [α-^{32}P]dATP and DNA synthesis was quantified. The time at which label and chase nucleotides were added is indicated by arrows. (**C**) Representative fibres labelled early in two consecutive cell cycles (green = digoxigenin-dUTP and red = biotin-dATP), as detailed in (**A**). The faint, continuous green line in the first panel corresponds to whole DNA stained with YOYO-1, the panel just below represents the same fibre (different contrast enhancement). Three different types of ETED (ETEDdig, ETEDbio, ETEDdigbio) were measured, as indicated above the images; bar = 10 kb. (**D**) Distributions of ETED between origins activated in the first S phase only (ETEDdig, green circles), second S phase only (ETEDbio, red squares) and between origins activated in the two consecutive S phases (all ETED or ETEDdigbio, blue diamonds).

distances (ETED) should be the same whether a single or both labels are scored. Finally, if clusters did not coincide more than expected by chance, an intermediary change, depending on the degree of origin clustering and cluster activation, should be observed. We found that the three distributions were fairly similar to each other (Figure 4D). The ETEDdigbio (mean = 15.4 kb) were only marginally shifted towards shorter distances

compared with the ETEDdig (mean = 16.9 kb, Table 1) or the ETEDbio (mean = 24.3 kb). The ETEDbio had a broader distribution than ETEDdig, consistent with a lower replication extent. The overall fork density was increased to the expected extent (Table 1). We conclude that origin clusters coincide neither more nor less than expected by chance between two cell cycles.

Table 1. Replication parameters of the first (digoxigenin labelling) and second (biotin labelling) S phases and analysis of green and red labels interspersion (digoxigenin and biotin)

	Digoxigenin labelling	Biotin labelling	Digoxigenin and biotin
Total no. of selected fibres	75	75	
Mean fibre length (kb)	94	94	
Total DNA length (kb)	7021	7021	
Total incorporation (kb)	857	600	
Incorporation extent	12.2	8.3	
Total no. of replication eyes	207	138	
Mean eye length (kb)	3.18	3.75	
Total no. of replication forks	453	292	745
Fork density (kb)	1/15.5	1/24	1/9.4
Total no. of ETED	143	70	269
Mean ETED (kb)	16.91	24.28	15.38

Thus, the timing of DNA replication is stochastic at the level of individual replicons and replicon clusters in *Xenopus* egg extracts.

Spatio-temporal replication programme of the rDNA domain

So far the replication programme was analysed on the whole genome level without distinguishing specific sequences. We therefore intended to study the timing programme at the rDNA repeat region, spanning 4 Mb on chromosome XII in *Xenopus laevis*. Replication of the rDNA locus in pre-MBT *Xenopus* embryos has been studied by 2D gel electrophoresis (12,16). Replication bubbles were detected everywhere along the rDNA repeat. Here, we re-investigated the distribution of initiation events along the rDNA repeat on single DNA fibres by DNA combing. Sperm chromatin replicating in egg extracts was labelled with digoxigenin–dUTP (t = 0–30 min), the DNA was purified and combed and the digoxigenin–labelled replication bubbles were detected with green fluorescent antibodies. The combed DNA was hybridized with a biotin-labelled fragment comprising the 3′ two-thirds of the rDNA transcription unit (probe B, Figure 5A) to reveal the rDNA repeats in red (Figure 5B). Initiation events were observed both within

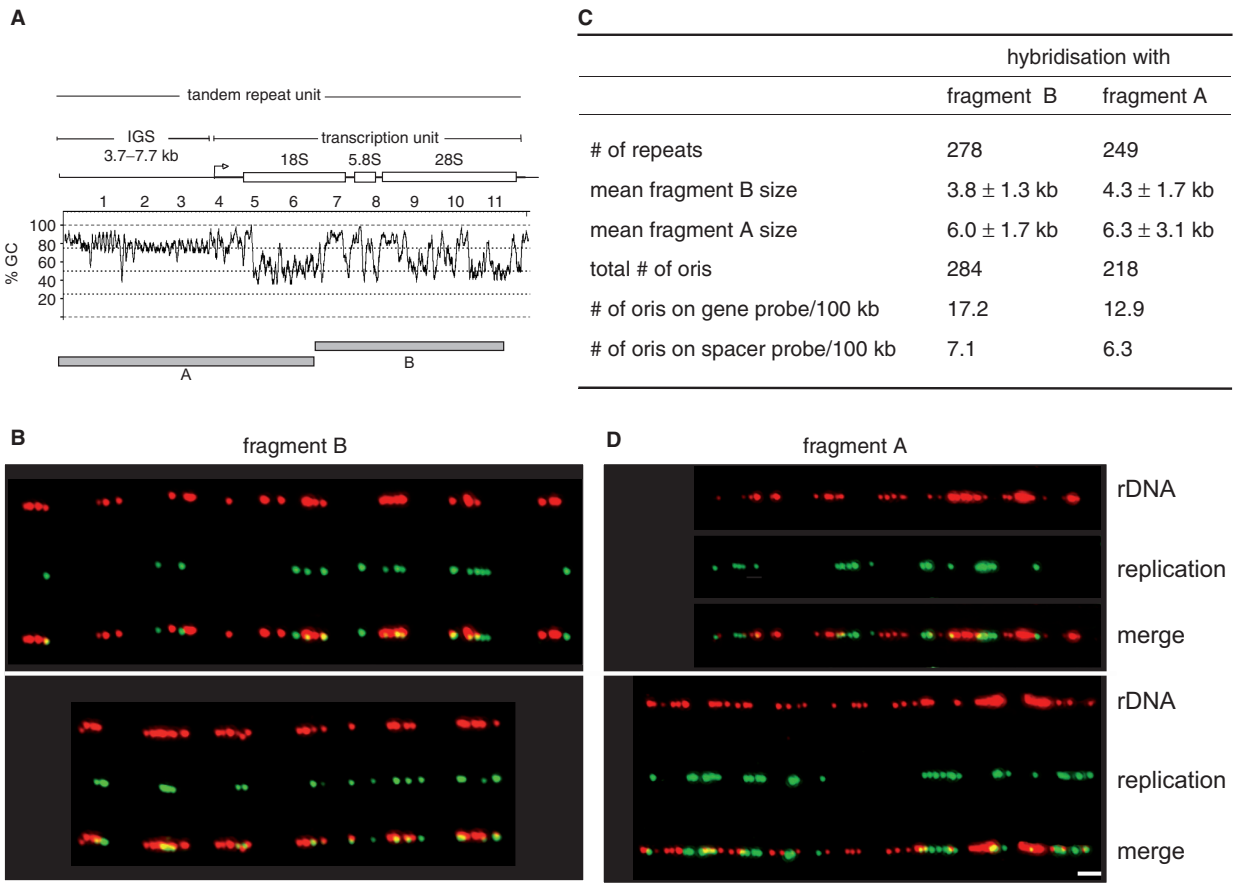

Figure 5. Preferential initiation in the transcription unit of the rDNA repeat. (**A**) Map of the *X. laevis* rDNA repeat and localization of probe B and A (grey boxes), GC plot with 55 bp sliding window; IGS, intergenic spacer. (**B** and **D**) Sperm nuclei were labelled for 30 min with digoxigenin–dUTP to mark replication eyes (in green) and combed DNA fibres were hybridized with biotinylated probe B (**B**) or probe A (**D**) (red); bar = 3 kb. (**C**) Origin counts on probe B and on the rest of the repeat (fragment A) and on probe A and the rest of the repeat (fragment B). A total of 5 Mb of rDNA was analysed.

and outside fragment B, with a mean spacing of 9.4 kb, as expected. However, the frequency of replication initiation normalized to DNA length was 2.5-fold higher in fragment B than in the rest of the repeat (17.2 versus 7.1 events per 100 kb; $P < 0.001$; Figure 5C). As hybridization might have interfered with the detection of replication signals we also used a probe against the intergenic spacer of the transcription unit (Figure 5D) and analysed the distribution of initiation events on DNA fibres labelled with digoxigenin–dUTP (Figure 5C). Consistently, we found twice less initiations in the spacer region than in the gene region (6.3 versus 12.9 events per 100 kb; $P < 0.001$; Figure 5C). Similar results were obtained in a second independent experiment using the same two probes and in an experiment using a third probe against the 5′-end of transcription unit (data not shown). The intergenic spacer sequence is known to be very GC-rich (27). Since it has been reported that *Xenopus* origin recognition complex (ORC) preferentially binds to AT-rich sequences (28), we compared the GC/AT content of the intergenic spacer with the coding region. The sequences of the two regions have a different GC/AT content (IGS: 78%; transcription unit: 67.3% GC; Figure 5A). Overall, these results demonstrate a higher frequency of initiation in the transcription unit than in the intergenic spacer. We conclude that initiation in the rDNA repeat unit is not completely random before MBT in the absence of transcription.

In order to determine the replication timing of the rDNA sequences relative to whole genome sequences, we compared the mean replication extent of the rDNA with that of the whole genome by summing the length of the bubbles and dividing by the total length of the respective DNA molecules. For this experiment, sperm nuclei were labelled with biotin–dUTP, stopped early and midway through S phase. Biotin-labelled replication bubbles were visualized in red. The rDNA (Figure 6A) was visualized by hybridization with a B fragment probe labelled by digoxigenin (in green). The whole genomic DNA was visualized using an anti-guanosine antibody (not shown). The replication extent of the rDNA was significantly lower than the replication extent of the whole genome in both early and mid S phase (Figure 6B: early S, 6.2% versus 11.5%, $P < 0.05$; mid S, 53.2% versus 64.4%, $P < 0.01$). Although the ETED (mean 7.5 kb versus 8 kb) and eye sizes (1.1 kb versus 1.2 kb) in early S phase were similar, the overall density of forks was lower in the rDNA than in the whole genome (9.5 versus 15.9 forks/100 kb) in early S phase. This suggests that origins in the rDNA are activated in clusters, as in the bulk of the genome, but at a slower pace.

A positive correlation between replication timing and chromatin structure on the level of large domains has been established in *Drosophila* and human differentiated cells (6,29). Although there is no clear distinction between eu- and hetero-chromatin in embryonic cells we analysed the chromatin structure of sperm nuclei assembled in egg extracts in the absence of DNA replication both at the rDNA locus and the whole genome by micrococcal nuclease digestion (Figure 6C). The rDNA was detected with a full-length repeat probe. Whereas genomic DNA showed a typical nucleosomal ladder, rDNA sequences were largely resistant to MNase digestion. Identical digestion patterns were obtained when chromatin was allowed to replicate (data not shown). Our results suggest that ribosomal chromatin has a different structure from the bulk of the genome even at the earliest developmental stage, when transcription does not occur.

We conclude that the spatio-temporal replication programme at the rDNA locus in early *Xenopus* embryos is not completely stochastic but might be regulated by transcription independent chromatin structures.

DISCUSSION

In this study we investigated whether the replication timing of specific sequences is regulated in the embryonic *Xenopus in vitro* system. We found that at the level of single replicons and replicon clusters replication timing is random since sequences replicated early in the first S phase do not coincide with sequences replicated early in the second S phase. But contrary to what was expected, the replication timing of large domains is not completely stochastic because early replication foci coincided in two consecutive cell cycles and timing of the large rDNA domain compared to bulk DNA replication was delayed. This is the first example of replication timing in the absence of specific initiation sites and transcription in eukaryotes.

Replication timing of whole genome sequences in *Xenopus* on the replicon, cluster and domain level

The time of activation of origin clusters and the firing of origins within clusters is dependent on the ATR/ATM checkpoint in the absence of induced DNA damage or stalled forks (20,25). This raised the question whether specific sequences replicate according to a reproducible timing programme or whether their activation is random. Our results show a lack of coincidence between origins fired in two successive cycles which is consistent with earlier data showing that initiation of DNA replication is random in early *Xenopus* embryos (12–14). This situation contrasts with somatic mammalian cells where previous DNA fibre studies have shown a colocalization of initiation sites in two consecutive S phases (30,31). However, it has been reported that there is no significant correlation between origin activation in two successive S phases in *Schizosaccharomyces pombe*, where initiation occurs at specific sequences (32). Recently, stochastic replication timing in *Saccharomyces cerevisiae* on the level of single origins on chromosome VI was reported (4). Our data suggest that any epigenetic marks that might play a role in origin timing specification are not transmitted from one cycle to the next in *Xenopus* egg extracts.

Although the time of activation of origins and origin clusters seems to be random, this does not appear to be the case for large domains such as replication foci. We found that replication foci are sequentially activated in sperm nuclei although stage-specific intranuclear patterns like in somatic cells (5) were not detected. However, a strong coincidence of replication foci activated early in one cell

A

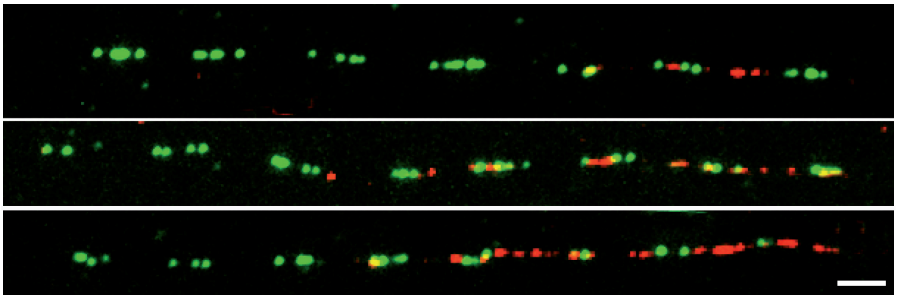

B

	Early S phase		Mid S phase	
	global DNA	rDNA repeats	global DNA	rDNA repeats
Total DNA measured	4730 kb	880 kb	4178 kb	3355 kb
DNA replicated	545 kb	43 kb	2692 kb	1784 kb
Replication extent	11.5 %	6.2 %	64.4 %	53.2 %

C

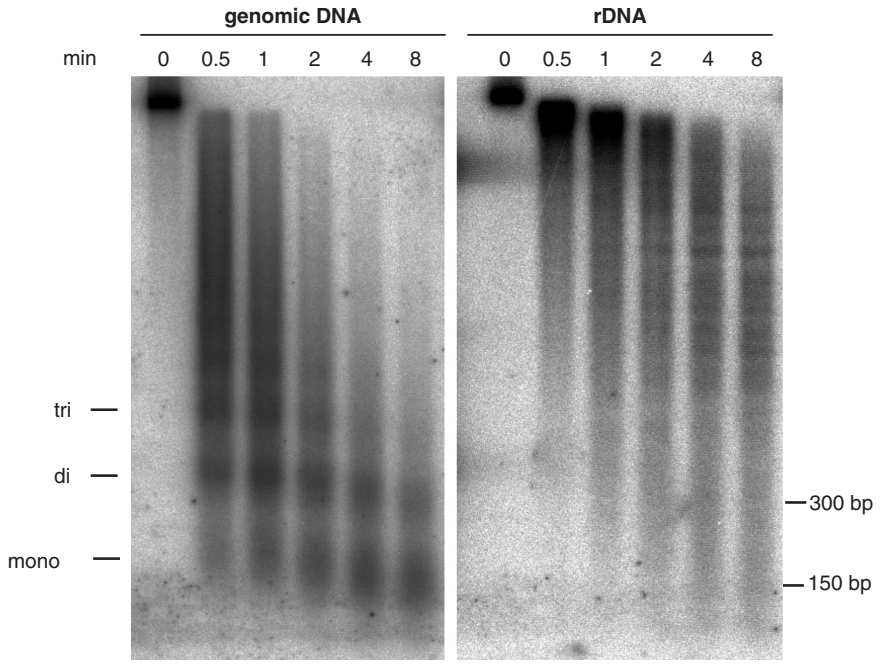

Figure 6. The rDNA replicates later than bulk genomic DNA and has a different chromatin structure. (**A**) Merged images of representative rDNA repeats in mid S phase. Green, rDNA probe; red: replication bubbles labelled by biotin-dUTP incorporation from 0 to 35 min and chased with dTTP (mid S phase), bar = 3 kb. (**B**) Replication extent of rDNA repeats and whole genomic DNA as analysed by combing. (**C**) Micrococcal digestion of sperm nuclei assembled in egg extracts in the presence of geminin. DNA was digested for the indicated time points, electrophoresed and hybridized either with a genomic DNA probe (left) or a full-length rDNA repeat probe (right). Positions of mono- and oligomeric nucleosomal DNA fragments are indicated on the left.

cycle with those also activated early in the next cell cycle was observed, similar to somatic cells. We found that ATR/ATM kinases do not appear to control the activation rate of replication foci but rather control the number of active replicons within active foci. It was recently reported that the pattern of replication foci is altered in chicken cells with compromised Chk1 or ATR activity (33) and in *S. pombe cds1* mutants (34). In human cells, however, no change in the number of replication foci was observed upon inhibition of either ATM/ATR with caffeine or Chk1 with UCN-01 (33). Our observations therefore appear to be more consistent with those reported in human cells.

The *Xenopus* rDNA repeat domain

By 2D gel analysis replication bubbles have been detected all over the rDNA repeat unit (16). Although we

confirmed that replication initiates everywhere in the tandem repeats we observed a 2-fold higher initiation rate in the rDNA transcription unit (67.3% GC) than in the intergenic spacer (78% GC) when the locus was analysed by molecular combing. The difference with the former study might be explained by a greater sensitivity of our single fibres approach in comparison to the DNA population based 2D gel analysis. The sharp difference in AT content between the spacer and the transcription unit may be responsible for the difference in initiation frequencies. In agreement with this hypothesis, it has been reported that addition of *S. pombe* Orc4, which binds to asymmetric AT sequences in *S. pombe*, inhibits DNA replication in the *Xenopus in vitro* system and that *Xenopus* ORC preferentially binds to AT-rich sequences (28). While our manuscript was under revision, an independent study was published which showed preferential initiation in asymmetric AT-rich sequences of λ phage DNA replicated in *Xenopus* egg extracts (35), supporting our observation in the *Xenopus* rDNA cluster.

The 400–600 copies of the rDNA repeat unit are all localized on the right arm of chromosome XII in *X. laevis* and span 4 Mb of DNA. Our results show that rDNA sequences are replicated later than bulk genomic DNA. In mammalian cells, transcriptionally inactive rDNA repeats are packaged in heterochromatin and replicate later than active repeat units (36). During early *Xenopus* development rDNA genes are not transcribed but their organization in prenucleolar bodies containing maternal pre-rRNAs has been reported (37). The observed resistance to MNase in our experiments suggests a more compact chromatin, and the lack of nucleosomal ladder suggests a non-nucleosomal or irregular nucleosomal structure. A similar MNase resistance of the *X. laevis* ribosomal chromatin was previously observed in adult blood and liver cells, where little or no transcription is occurring, and in stage 40 embryo cells, where these genes are fully transcribed (38). This less accessible chromatin structure might be one cause of the observed delay in rDNA replication. In addition, the preferential initiation at AT-rich sequences may result in an overall lower efficiency of initiation in the rDNA (overall 70% GC) than in the rest of the genome (42% GC), which might also be responsible for the delayed replication of the rDNA.

In conclusion, we have shown that the replication timing programme is not completely random in *Xenopus* egg extracts in the absence of transcription. Replication foci, which correspond to stable chromosome structural units of large size (~1 Mb), appear to fire in a reproducible sequence from one S phase to the next. This defined pattern may be underlain by large-scale differences in chromatin structure. The rDNA locus (~4 Mb) appears to replicate on average later than the bulk of the genome, and this coincides with a particularly inaccessible chromatin structure. Once a replication focus is activated, however, origins and origin clusters within it are activated in a stochastic manner and epigenetic marks on origins are not transferred from one cycle to the next (Figure 7). Several studies in *Drosophila* (6) and human cells (39–41) positively correlated transcriptional status and replication time over broad regions (>100 kb). It is unclear whether active transcription promotes early replication or vice versa. Plasmid injection experiments at different stages of S phase revealed that replication timing is necessary for propagating active or repressive chromatin structures to the next cell cycle (42). Our results in the transcriptionally inactive embryonic *Xenopus* system suggest that replication timing of large regions might be dependent on large-scale features of chromosome structure suggesting that basic replication timing is established prior to the transcriptional activity during early development. It will be interesting to test this hypothesis in future *in vivo* experiments.

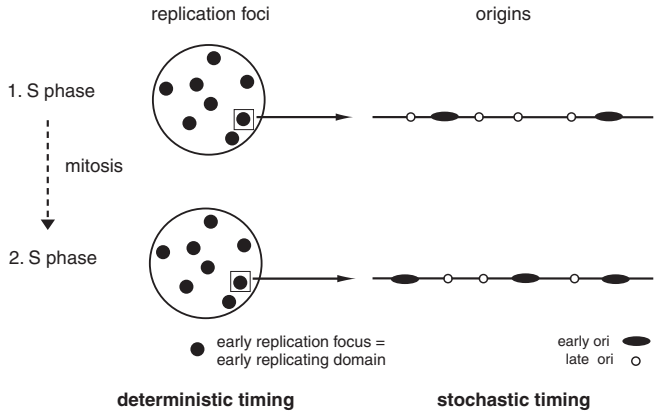

Figure 7. Model of replication timing in the *Xenopus in vitro* system. Replication timing is maintained during subsequent S phases at the level of replication foci and large chromatin domains, but not at the level of replication origins.

ACKNOWLEDGEMENTS

We thank Arach Goldar and Vincent Gaggioli for helpful advices and discussions, Torsten Krude and Chrystelle Maric for critical reading of the manuscript.

FUNDING

The Ligue Contre le Cancer (Comité de Paris) (O.H.); Association pour la Recherche sur le Cancer (O.H.); Agence Nationale pour la Recherche (O.H.). MENESR fellowship (H.L and T.G.); Association pour la Recherche sur le Cancer (H.L. and T.G.). Funding for open access charge: CNRS.

Conflict of interest statement. None declared.

REFERENCES

1. Sclafani,R.A. and Holzen,T.M. (2007) Cell cycle regulation of DNA replication. *Annu. Rev. Genet.*, **41**, 237–280.
2. Lucas,I.A. and Raghuraman,M.K. (2003) The dynamics of chromosome replication in yeast. *Curr. Top. Dev. Biol.*, **55**, 1–73.
3. Raghuraman,M.K., Winzeler,E.A., Collingwood,D., Hunt,S., Wodicka,L., Conway,A., Lockhart,D.J., Davis,R.W., Brewer,B.J. and Fangman,W.L. (2001) Replication dynamics of the yeast genome. *Science*, **294**, 115–121.

4. Czajkowsky,D.M., Liu,J., Hamlin,J.L. and Shao,Z. (2008) DNA combing reveals intrinsic temporal disorder in the replication of yeast chromosome VI. *J. Mol. Biol.*, **375**, 12–19.
5. Zink,D. (2006) The temporal program of DNA replication: new insights into old questions. *Chromosoma*, **115**, 273–287.
6. MacAlpine,D.M., Rodriguez,H.K. and Bell,S.P. (2004) Coordination of replication and transcription along a Drosophila chromosome. *Genes Dev.*, **18**, 3094–3105.
7. Dimitrova,D.S. and Gilbert,D.M. (1999) The spatial position and replication timing of chromosomal domains are both established in early G1 phase. *Mol. Cell*, **4**, 983–993.
8. Wu,J.R. and Gilbert,D.M. (1996) A distinct G1 step required to specify the Chinese hamster DHFR replication origin. *Science*, **271**, 1270–1272.
9. Rhind,N. (2006) DNA replication timing: random thoughts about origin firing. *Nat. Cell Biol.*, **8**, 1313–1316.
10. Newport,J. and Kirschner,M. (1982) A major developmental transition in early Xenopus embryos: I. characterization and timing of cellular changes at the midblastula stage. *Cell*, **30**, 675–686.
11. Mills,A.D., Blow,J.J., White,J.G., Amos,W.B., Wilcock,D. and Laskey,R.A. (1989) Replication occurs at discrete foci spaced throughout nuclei replicating in vitro. *J. Cell Sci.*, **94**(Pt 3), 471–477.
12. Hyrien,O. and Mechali,M. (1993) Chromosomal replication initiates and terminates at random sequences but at regular intervals in the ribosomal DNA of Xenopus early embryos. *EMBO J.*, **12**, 4511–4520.
13. Hyrien,O. and Mechali,M. (1992) Plasmid replication in Xenopus eggs and egg extracts: a 2D gel electrophoretic analysis. *Nucleic Acids Res.*, **20**, 1463–1469.
14. Mahbubani,H.M., Paull,T., Elder,J.K. and Blow,J.J. (1992) DNA replication initiates at multiple sites on plasmid DNA in Xenopus egg extracts. *Nucleic Acids Res.*, **20**, 1457–1462.
15. Lucas,I., Chevrier-Miller,M., Sogo,J.M. and Hyrien,O. (2000) Mechanisms ensuring rapid and complete DNA replication despite random initiation in Xenopus early embryos. *J. Mol. Biol.*, **296**, 769–786.
16. Hyrien,O., Maric,C. and Mechali,M. (1995) Transition in specification of embryonic metazoan DNA replication origins. *Science*, **270**, 994–997.
17. Blow,J.J., Gillespie,P.J., Francis,D. and Jackson,D.A. (2001) Replication origins in Xenopus egg extract are 5–15 kilobases apart and are activated in clusters that fire at different times. *J. Cell Biol.*, **152**, 15–25.
18. Herrick,J., Stanislawski,P., Hyrien,O. and Bensimon,A. (2000) Replication fork density increases during DNA synthesis in X. laevis egg extracts. *J. Mol. Biol.*, **300**, 1133–1142.
19. Marheineke,K. and Hyrien,O. (2001) Aphidicolin triggers a block to replication origin firing in Xenopus egg extracts. *J. Biol. Chem.*, **276**, 17092–17100.
20. Marheineke,K. and Hyrien,O. (2004) Control of replication origin density and firing time in Xenopus egg extracts: role of a caffeine-sensitive, ATR-dependent checkpoint. *J. Biol. Chem.*, **279**, 28071–28081.
21. Jun,S., Herrick,J., Bensimon,A. and Bechhoefer,J. (2004) Persistence length of chromatin determines origin spacing in Xenopus early-embryo DNA replication: quantitative comparisons between theory and experiment. *Cell Cycle*, **3**, 223–229.
22. Germe,T. and Hyrien,O. (2005) Topoisomerase II-DNA complexes trapped by ICRF-193 perturb chromatin structure. *EMBO Rep.*, **6**, 729–735.
23. Anglana,M., Apiou,F., Bensimon,A. and Debatisse,M. (2003) Dynamics of DNA replication in mammalian somatic cells: nucleotide pool modulates origin choice and interorigin spacing. *Cell*, **114**, 385–394.
24. Esposito,A., Dohm,C.P., Kermer,P., Bahr,M. and Wouters,F.S. (2007) Alpha-Synuclein and its disease-related mutants interact differentially with the microtubule protein tau and associate with the actin cytoskeleton. *Neurobiol. Dis.*, **26**, 521–531.
25. Shechter,D. and Gautier,J. (2004) MCM proteins and checkpoint kinases get together at the fork. *Proc. Natl Acad. Sci. USA*, **101**, 10845–10846.
26. Hutchison,C.J., Cox,R. and Ford,C.C. (1988) The control of DNA replication in a cell-free extract that recapitulates a basic cell cycle in vitro. *Development*, **103**, 553–566.
27. Boseley,P., Moss,T., Machler,M., Portmann,R. and Birnstiel,M. (1979) Sequence organization of the spacer DNA in a ribosomal gene unit of Xenopus laevis. *Cell*, **17**, 19–31.
28. Kong,D., Coleman,T.R. and DePamphilis,M.L. (2003) Xenopus origin recognition complex (ORC) initiates DNA replication preferentially at sequences targeted by Schizosaccharomyces pombe ORC. *EMBO J.*, **22**, 3441–3450.
29. Birney,E., Stamatoyannopoulos,J.A., Dutta,A., Guigo,R., Gingeras,T.R., Margulies,E.H., Weng,Z., Snyder,M., Dermitzakis,E.T., Thurman,R.E. *et al.* (2007) Identification and analysis of functional elements in 1% of the human genome by the ENCODE pilot project. *Nature*, **447**, 799–816.
30. Jackson,P.K., Chevalier,S., Philippe,M. and Kirschner,M.W. (1995) Early events in DNA replication require cyclin E and are blocked by p21CIP1. *J. Cell Biol.*, **130**, 755–769.
31. Li,F., Chen,J., Solessio,E. and Gilbert,D.M. (2003) Spatial distribution and specification of mammalian replication origins during G1 phase. *J. Cell Biol.*, **161**, 257–266.
32. Patel,P.K., Arcangioli,B., Baker,S.P., Bensimon,A. and Rhind,N. (2006) DNA replication origins fire stochastically in fission yeast. *Mol. Biol. Cell*, **17**, 308–316.
33. Maya-Mendoza,A., Petermann,E., Gillespie,D.A., Caldecott,K.W. and Jackson,D.A. (2007) Chk1 regulates the density of active replication origins during the vertebrate S phase. *EMBO J.*, **26**, 2719–2731.
34. Meister,P., Taddei,A., Ponti,A., Baldacci,G. and Gasser,S.M. (2007) Replication foci dynamics: replication patterns are modulated by S-phase checkpoint kinases in fission yeast. *EMBO J.*, **26**, 1315–1326.
35. Stanojcic,S., Lemaitre,J.M., Brodolin,K., Danis,E. and Mechali,M. (2008) In Xenopus egg extracts DNA replication initiates preferentially at or near asymmetric AT sequences. *Mol. Cell Biol.*, doi:101128/MCB.00181-08.
36. Li,J., Santoro,R., Koberna,K. and Grummt,I. (2005) The chromatin remodeling complex NoRC controls replication timing of rRNA genes. *EMBO J.*, **24**, 120–127.
37. Verheggen,C., Le Panse,S., Almouzni,G. and Hernandez-Verdun,D. (1998) Presence of pre-rRNAs before activation of polymerase I transcription in the building process of nucleoli during early development of Xenopus laevis. *J. Cell Biol.*, **142**, 1167–1180.
38. Spadafora,C. and Crippa,M. (1984) Compact structure of ribosomal chromatin in Xenopus laevis. *Nucleic Acids Res.*, **12**, 2691–2704.
39. White,E.J., Emanuelsson,O., Scalzo,D., Royce,T., Kosak,S., Oakeley,E.J., Weissman,S., Gerstein,M., Groudine,M., Snyder,M. *et al.* (2004) DNA replication-timing analysis of human chromosome 22 at high resolution and different developmental states. *Proc. Natl Acad. Sci. USA*, **101**, 17771–17776.
40. Woodfine,K., Beare,D.M., Ichimura,K., Debernardi,S., Mungall,A.J., Fiegler,H., Collins,V.P., Carter,N.P. and Dunham,I. (2005) Replication timing of human chromosome 6. *Cell Cycle*, **4**, 172–176.
41. Karnani,N., Taylor,C., Malhotra,A. and Dutta,A. (2007) Pan-S replication patterns and chromosomal domains defined by genome-tiling arrays of ENCODE genomic areas. *Genome Res.*, **17**, 865–876.
42. Zhang,J., Xu,F., Hashimshony,T., Keshet,I. and Cedar,H. (2002) Establishment of transcriptional competence in early and late S phase. *Nature*, **420**, 198–202.